Articles

Characterizing hydrocarbon discoveries and prospects in the Tay Sandstone using relative elastic inversion: Greater Pilot area, Central North Sea

David Went,[1]* Maurice Bamford,[2] Jon Rogers,[1] Stephen Brown[2] and Graham Turner[1]

[1]TGS Geophysical Company ASA, Dukes Court, Woking GU21 5BH, UK
[2]Orcadian Energy PLC, 6th Floor, 60 Gracechurch Street, London EC3V 0HR, UK
DW, 0000-0001-8049-4247
*Correspondence: david.went@tgs.com

Abstract: The Pilot oil accumulation and associated discoveries of Blocks 21/27 and 21/28 have been stranded assets for three decades. The principal cause of delay in developing the oil fields is because these are heavy oils with low gas–oil ratio and, in some cases, significant gas caps. The oil in the Tay Sandstone is trapped in structural and stratigraphic closures at a depth of 800–1300 m. Determining pay thickness and delimiting oil-in-place in some existing discoveries and especially in undrilled prospects has been problematic. This difficulty has been addressed by conducting an innovative amplitude versus offset (AVO) inversion of the seismic data which has been successfully blind tested against the wells and prognosed closures. The method, which is a band-limited form of extended elastic impedance (EEI), has proved robust for discriminating gas-, oil- and brine-filled sands from one another. Oil and gas trapped further down-dip in the discoveries Fyne, Crinan and Dandy are developed in Tay reservoirs showing generally lower net-to-gross. The sensitivity of the rEEI attribute to the presence of thicker intervals of oil pay, in this case, is used to indicate where higher net-to-gross is present above the oil–water contact, a characteristic of direct relevance to the planning of optimally located development wells.

The Pilot oil accumulation and associated discoveries in Blocks 21/27 and 21/28 have been stranded assets for up to three decades (Fig. 1). There has been a delay in developing these oil accumulations because they are either heavy oils with low gas–oil ratio (GOR), or the oil is present in reservoirs with ill-defined closures or showing low net-to-gross. The challenge in developing the discoveries is an integrated one involving both geoscience and engineering. The oil in the Tay Sandstone Member (Tay) is typically trapped in structural and stratigraphic closures, the latter commonly having a structural component, at a depth of 800–1300 m. The oil-in-place is relatively well delimited in those discoveries with high net-to-gross reservoirs, but much less so in the lower net-to-gross pools. Having seven reservoir penetrations on Pilot has helped. Despite this, challenges still exist on the pinch-out margin and in areas where the amplitude response is more variable.

Another challenge is the identification and de-risking (or high-grading) of additional undrilled prospective resources. Building an understanding of the critical accessible volume of oil-in-place in individual accumulations and in the broader area is fundamental to commercialization of the resources present in the region. Seismic data are critical to mapping the extent of oil-in-place. However, the combination of oil and reservoir properties makes discrimination of oil from water difficult using the stack seismic data alone. Examination of rock and oil properties from well logs suggested elastic inversion of the seismic data may be of help in this regard and provided the motivation to conduct inversion studies on the data.

The objective of this paper is to show how elastic inversion has been used to: (1) delineate oil distribution in existing Tay discoveries; (2) define sand and hydrocarbon migration fairways; (3) highlight areas of higher net-to-gross in generally low net-to-gross Tay reservoirs; and (4) identify and high-grade new prospects.

Geological setting and previous work

The study area (around Blocks 21/27 and 28) is located on the Western Platform of the Central Graben. It represents the relatively unfaulted rift margin to the Late Jurassic-aged graben, where Zechstein evaporites have produced halokinetic structures with salt 'intrusion' into the overlying Triassic and Jurassic stratigraphy. The overlying thermal subsidence sequence of Cretaceous, Paleogene and Neogene strata are relatively undisturbed, containing low amplitude structures from ongoing salt movement at depth.

The area contains several oil and gas discoveries in both structural and stratigraphic traps: namely Pilot, Harbour, Blakeney, Feugh, Dandy, Crinan and Fyne (Fig. 1). These are contained within the Eocene Tay reservoir (Fig. 2) at depths of 800–1300 m; reservoir depth generally increases from west to east. Overall, the oil properties reflect this with heavy oils present in the west and medium-gravity oils in the east. The change in specific oil gravity is attributed to increased biodegradation in the shallower section where reservoir temperatures are slightly lower. In Pilot and Blakeney the oil is relatively heavy with a gravity of 12–17°API and a GOR of *c.* 80 scf/bbl. The oil is lighter further to the east in Fyne where the gravity is 25°API and the GOR is *c.* 210 scf/bbl. Free gas is common but does not occur over all accumulations. Where sampled, it is virtually 100% methane, which is taken to be indicative of biodegradation from oil. The absence of gas caps in some accumulations is attributed to poor lateral seal in stratigraphic pinch-out traps (e.g. west of Pilot), crestal faulting and associated fracturing (e.g. Blakeney), and weak top seal to the south of our study area (e.g. Elke).

The Pilot oils have been typed to the Kimmeridge Clay Formation which is locally immature, and long-distance migration from the source kitchen in the Central Graben is required, *c.* 50 km in the case of Pilot. As hydrocarbons have migrated westwards from the kitchen, they have progressively migrated into chronologically younger reservoirs, until by Block 21/27, oil is only found in the uppermost sand package within the Tay Sandstone Member (Brown *et al.* 2020). There are no younger reservoir sands in the Tertiary in the area.

The Tay Sandstone Member forms the reservoir within the mudstone-dominated Horda Formation (Knox and Holloway 1992), and in chronostratigraphy and sequence stratigraphy terms, the Tay sandstone was deposited over a period of *c.* 10 Ma between sequences T60 and T94 (Jones *et al.* 2003). The Tay

From: Gill, C., Goffey, G. and Underhill, J. R. (eds) *Powering the Energy Transition through Subsurface Collaboration: Proceedings of the 1st Energy Geoscience Conference*. Geological Society, London, Energy Geoscience Conference Series, **1**, https://doi.org/10.1144/egc1-2023-37

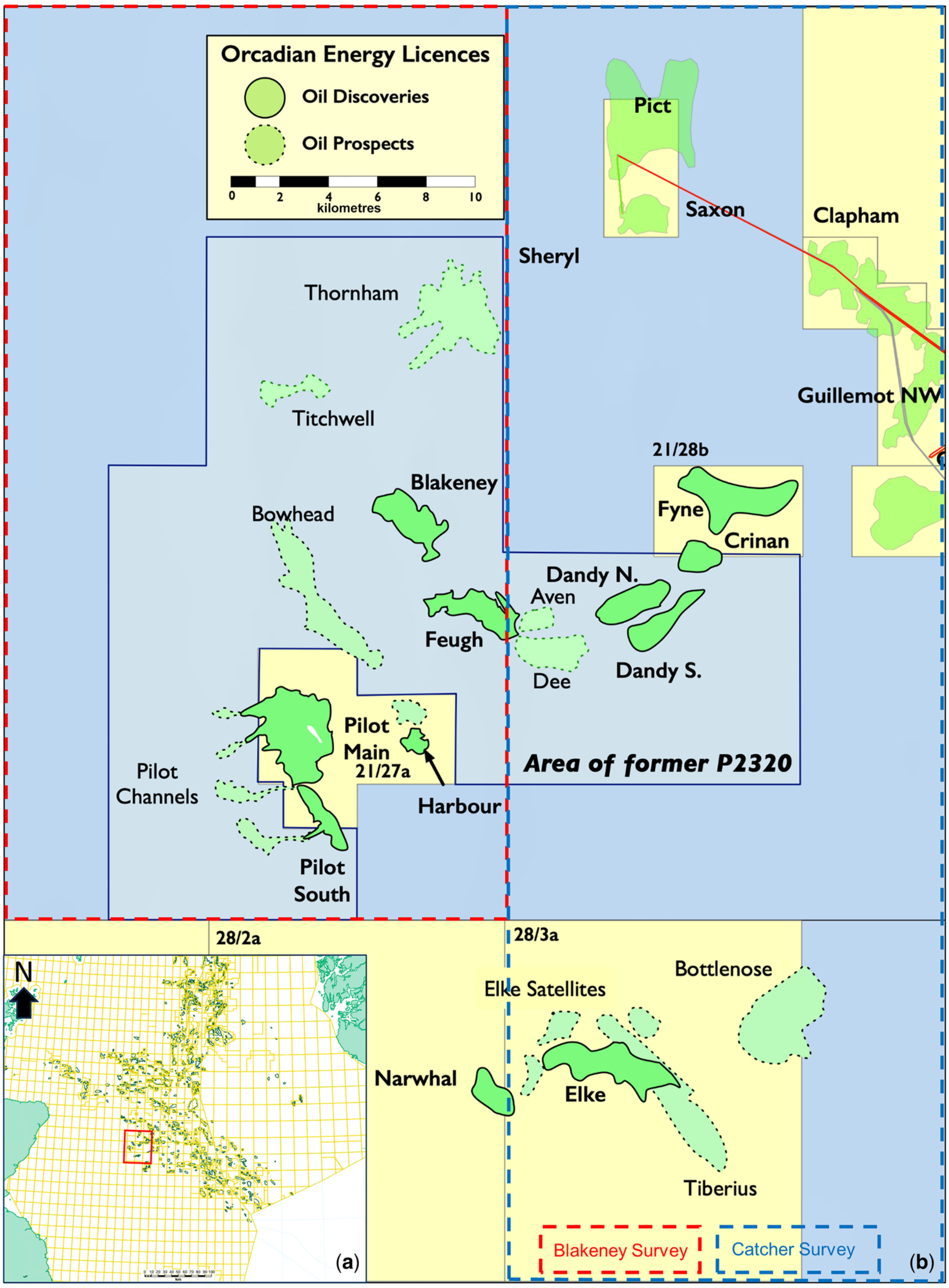

Fig. 1. Location of (**a**) study area and (**b**) fields, discoveries, prospects and surveys.

Sandstone Member is a stacked deep-water turbiditic sequence sitting to the east of the shallow-water Mousa Formation. The complete Tay sequence is time-equivalent to part of the Mousa Formation.

The Tay gross depositional environment map for the greater area (Fig. 3) illustrates the general distribution of Tay sands along with a number of distinct palaeogeographical areas.

(1) The Mousa Shelf or delta-top where shallow marine sediments contain sands, typically in a series of stacked cleaning-upward cycles; the area lacks any hydrocarbon discoveries.
(2) The Primary Slope is a prograding clinoform package (Figs 3 & 4) with localized narrow incised feeder canyons supplying sediment from the shelf into the basin.
(3) The Composite Terrace is a distinct generally sandy depositional area interpreted as lacking a significant depositional slope and resulted in deposition of perched or transient fan systems (Adeogba *et al.* 2005). The area contains the Upper Tay Sandstone C unit (also referred to informally as the PE3c, based on biostratigraphy) which is a lowstand, amalgamated sandbody forming a thick, high net-to-gross, excellent quality reservoir unit (see thick sandbody in Fig. 5) at the very top of the Tay Sandstone Member (Fig. 2). It is this unit that contains all of the oil discovered on the Composite Terrace. It is used to define the extent of the Composite Terrace, since the underlying units in the Tay Sandstone Member may not be high net-to-gross (e.g. Blakeney).
(4) The Secondary Slope represents an increase in depositional slope to the east, resulting in an area of mudstone deposition (Horda Formation) with composite channels containing significantly lower net-to-gross sand packages than seen in the Tay Sandstone Member of the Composite Terrace, and also lacking the Upper Tay Sandstone C (PE3c) reservoir unit. These channels are essentially bypass zones feeding sands to the basinal area.
(5) The Basin-floor fan area contains thick Tay sandstone packages with Lower, Middle and Upper Tay sands recognized; these units connect with the channels of the Secondary Slope.

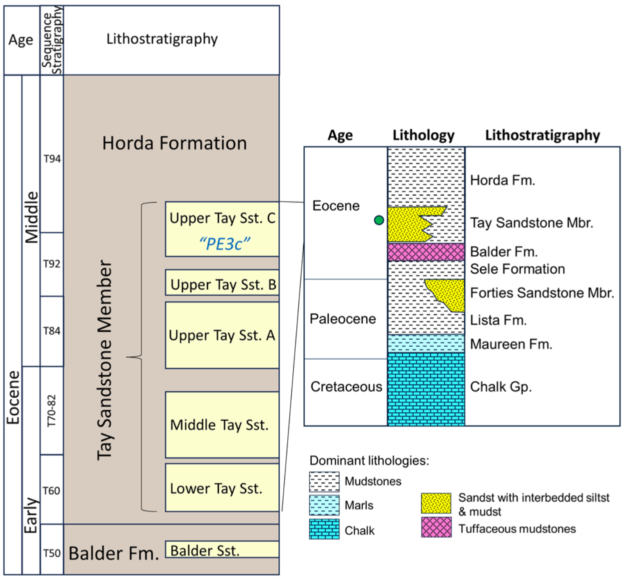

Fig. 2. Stratigraphic framework. Source: modified from Brown *et al.* (2020) and Jones *et al.* (2003).

These areas can be seen on seismic section (Fig. 4), though as a result of post-Tay deposition, halokinetic movement, subsidence and compaction, the Composite Terrace (transient basin) and Secondary Slope are difficult to distinguish from each other.

The Balder Formation Tuff has largely been reworked by the lowermost Tay system but is locally present in the more basinward parts of the study area. The underlying Paleocene strata are dominantly mudstones of the Maureen, Lista and Sele formations. The Forties Sandstone Member of the Sele Formation represents an axial draining submarine fan system and is present in more basinward localities, for example, around the Guillemot Field in the east of the study area. At the base of the Paleogene, the Top Chalk is the most prominent and easily mapped horizon in the study area, forming a pronounced trough in the stacked seismic section (Fig. 4).

Within the study area, the strata generally deepen to the ENE and this continues into the Western Trough of the Central Graben which was initially formed during Late Jurassic rifting, and then subsequently deepened through thermal subsidence. Within the study area, swells and troughs in the structure are superimposed on this general east-northeastwards deepening and are predominantly a result of halokinetic movements in the Zechstein evaporites. These movements are most pronounced during the Triassic and Jurassic but continue into the Eocene. This halokinesis results in the structural relief seen at top Tay level, helping form many of the closures or influencing Tay sedimentation which may set up stratigraphic traps (Brown *et al.* 2020) (Fig. 4).

Methods

The area of interest contains 27 exploration and appraisal wells, drilled during the period 1967 to 2011. A standard suite of wireline logs (gamma ray, resistivity, neutron, density, P-sonic) are present in most wells, but shear sonic logs are scarce (present in four wells). Available wireline logs from the wells have been examined and processed geologically and petrophysically. An example of the well processing is shown in Figure 5 from the Blakeney discovery well 21/27b-7, which has a shear sonic log. The figure shows the typical responses of logs through the section containing the Tay reservoir in the Pilot–Blakeney area. The logs are processed to show a display summarizing lithology, porosity and fluid type/saturation, which may be compared with the seismic property curves of acoustic impedance and extended elastic impedance (EEI); in this case EEIχ27 is used and is justified in the succeeding paragraph. The acoustic impedance log shows negligible deviation through the section, suggesting this seismic attribute would be of little or no use in lithology and fluid prediction. The EEIχ27 curve, on the other hand, shows a distinct lowering of values through the oil leg suggesting it may help detect the presence of oil directly in the Tay. Brine-filled sandstone is not easily distinguished from shale using either acoustic impedance or elastic impedance.

The lack of shear wave log data is not unusual but raises the question of whether the sparsely acquired shear wave data are fully representative of the rocks drilled. Comparison of the V_p/V_s relationships, determined from the few wells with measured shear wave data in the study area, compares favourably with globally

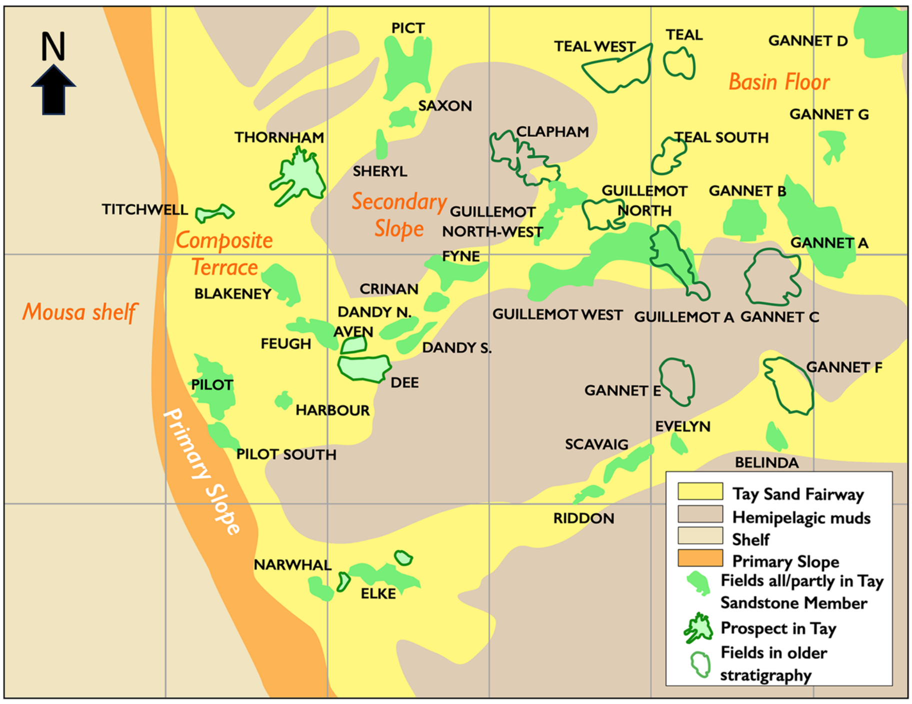

Fig. 3. Gross depositional environment inferred from well, seismic reflection and seismic inversion data. The shelf (buff) and slope (orange) represent the top and slope of the Mousa 'delta'. Dee and Thornham are high-graded prospects that lie at the transition between the foot of Mousa platform and the slope channel fairways.

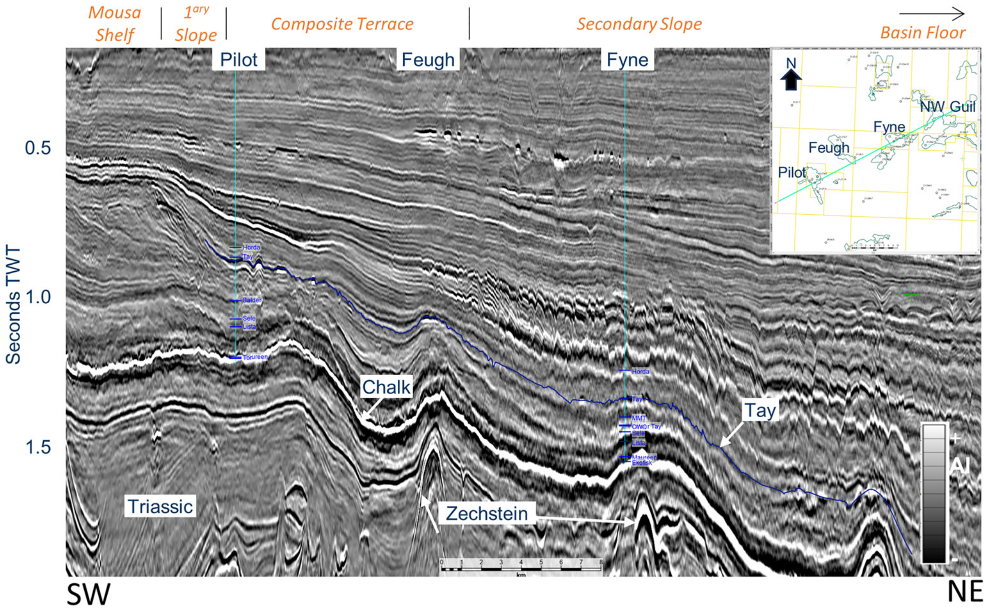

Fig. 4. Arbitrary line through the study area showing the level of the top Tay Sandstone Member, top Chalk and Zechstein salt swells. Tay–Mousa depositional areas are annotated along the top of seismic line.

observed trends for siliciclastic lithologies and their resulting empirical estimators (e.g. Greenberg and Castagna 1992; Vernik 2016; Mur and Vernik 2019). Together they suggest that the data probably are robust and that hydrocarbons should be optimally discriminated from shale and brine sandstone using a projection of intercept–gradient data to an incidence angle of *c.* 45° (Went 2021). This is equivalent to a rotation angle of 27° on an intercept-gradient cross-plot, since $\sin^2\theta = \tan\chi$ (Fig. 6). Although sandstone can commonly be discriminated from shale using the same rotation angle (Went 2021), the wireline data in this case suggest it will not be possible, probably due to the shallow depth of the target. At shallow depths compaction is limited and the elastic properties of sand and shale are more similar than they are at greater depth.

The seismic input to this study comprised two surveys: the Blakeney survey, acquired in 2011 and reprocessed in 2019; and the Catcher survey acquired between 2011 and 2013 and reprocessed in 2022. All these surveys were acquired in a standard narrow azimuth (NAZ) configuration and processed through a pre-stack time migration sequence utilizing the latest in deghosting, demultiple and regularization techniques. The Catcher reprocessing employed migrated sub-volumes through the lifetime of the project to confirm

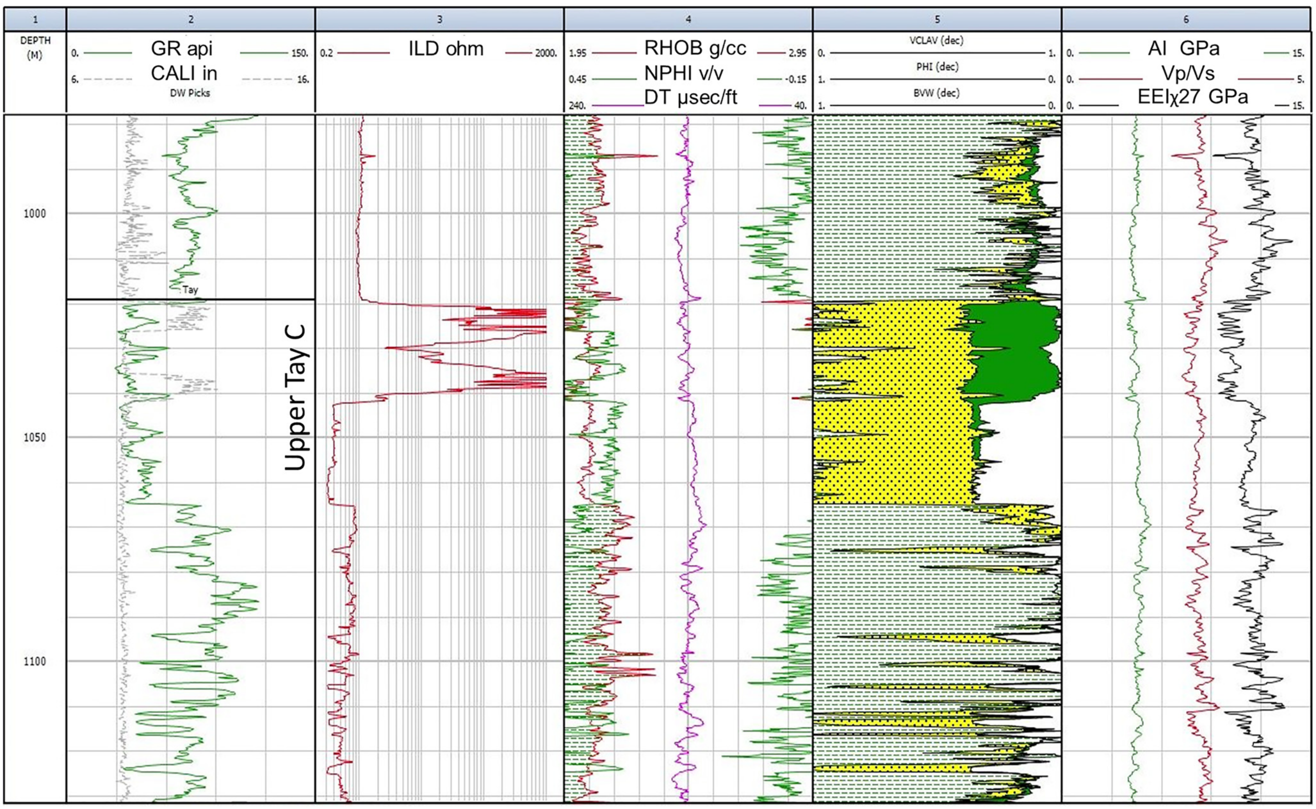

Fig. 5. Well logs and petrophysical interpretation from Blakeney well 21/27b-7. There is little in the way of change in the acoustic impedance log through the oil leg in the well, whereas a significant drop in the EEIχ27 log curve values suggests it may be of use in discriminating oil- from water-bearing sandstones.

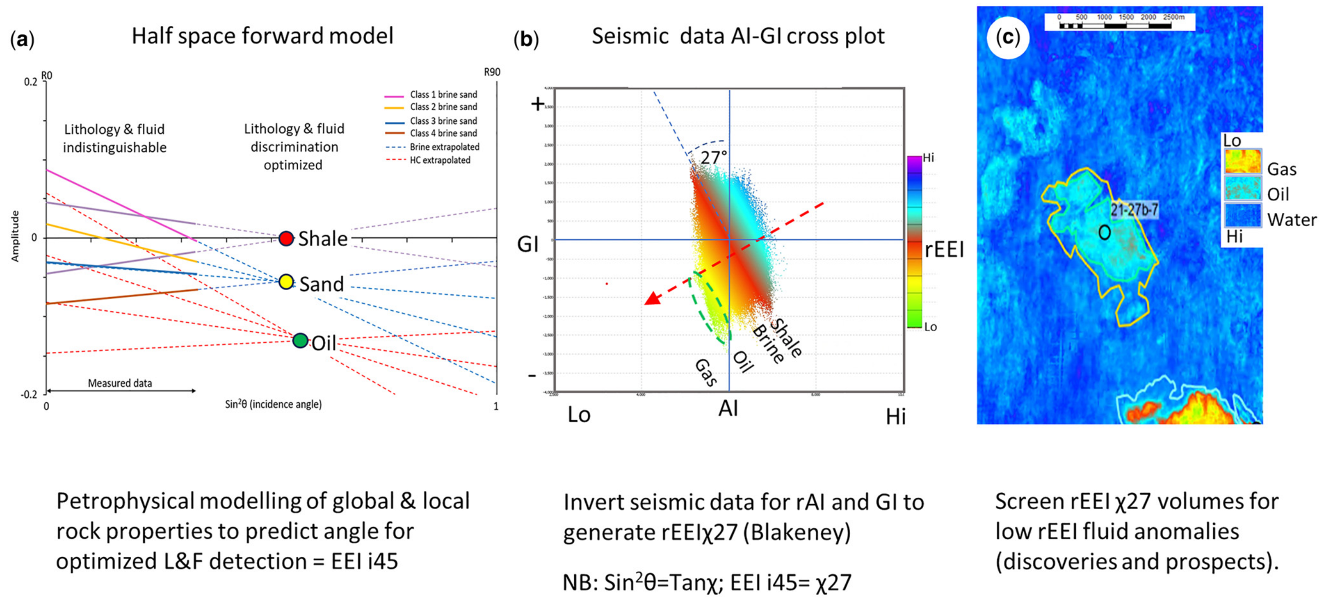

Fig. 6. Workflow summary: (**a**) rock property I–G trends, plotted as $\sin^2\theta$ (incidence angle) v. reflection coefficient, to predict angles for optimal lithology and fluid detection; (**b**) inversion of the seismic data for AI, GI and rEEIχ27, in this case displayed as a cross-plot of a cube of data over the Blakeney discovery; and (**c**) horizon slice of the attribute rEEIχ27 from a window around Top Tay (−5 to +20 ms) that shows the geographical extent of anomalously low values that may be attributed to the presence of oil and gas. The rEEIχ27 horizon slice shows the Blakeney anomaly conforming to the closing contour, with oil confirmed by well 21/27b-7. Source: (a) after Went (2021).

the consistency compared to Blakeney and to ensure a seamless final merge. The resultant high quality broadband dataset, achieving frequencies up to 75 Hz at the Tay reservoir level, was subdivided into partial angle stacks (near 5–14°, far 32–41°) as input to the elastic inversion.

Our preferred method of inverting seismic data to achieve the goal of using intercept and gradient (I&G) data, is to do it in impedance units rather than as amplitude from reflection data directly (Table 1). Such a process removes tuning artefacts, stabilizes gradient estimates and trace-math calculations, and simplifies the interpretation. Hence, intercept becomes intercept-impedance or acoustic-impedance (AI), whereas gradient becomes gradient-impedance (GI). Extended elastic impedance is a mathematical combination of AI and GI (Whitcombe *et al.* 2002). Although our preference is to work in impedance space, we want the seismic data to 'speak' for themselves. For this reason, no well data, low frequency trend or horizons are included in the impedance inversion. The output product is therefore relative extended elastic impedance (rEEI) and, as the name suggests, it is a simple band-limited (or relative) inversion of the seismic data. This then allows the well data to be used as an independent check on the attribute accuracy in fluid prediction.

Figure 6b shows the result of this inversion over the Blakeney discovery in the form of an AI–GI cross-plot, colour coded for rEEIχ27. The rEEIχ27 attribute can be seen to be a 'look across' the intercept–gradient cross-plot. The oil in the Blakeney discovery is highlighted by the low rEEI values shown in green colours, which plot in a sector of the AI–GI cross-plot typical of Class 2 amplitude versus offset (AVO) anomalies (Rutherford and Williams 1989; Castagna and Swan 1997). Of note, whilst the oil displays an anomalous rEEIχ27 response compared to brine, it is not anomalous in terms of acoustic impedance alone; it shares the same acoustic impedance as much of the background brine data plotting in the yellow and red colours.

One of the advantages of using the attribute rEEIχ27 is that the user can screen areas for anomalies using a single volume rather than having to resort to cross-plotting I&G. In this sense, it builds on the concept of fluid factor (Smith and Gidlow 1987; Gidlow *et al.* 1993; Fatti *et al.* 1994). Figure 6c shows a horizon slice from Top Tay which illustrates the lower values of rEEIχ27 forming an anomaly that closely corresponds to the closing contour on the Blakeney four-way dip structure, with a spill point verified by the well data (Fig. 4). This close correspondence helps build confidence that the AVO in the seismic data is capable of discriminating fluid type in the Tay reservoir. The fact that the rEEI anomaly is smaller than the mapped outline is to be expected, since a critical thickness of oil column would be required to produce an anomaly.

Table 1. Method for generating rEEIχ27 (see also Went *et al.* 2023)

Input	Action	Output
Near angle stack (5–15°)	Relative impedance inversion	rEI 10°
Far angle stack (30–40°)	Relative impedance inversion	rEI 35°
rEI 10°, rEI 35°	Trace maths	GI, rAI
rAI, GI	Trace maths	rEEI θ45° (χ 27°)

Pilot–Blakeney area results

In the Pilot–Blakeney area, hydrocarbons are contained in the distinct amalgamated sandstone body at the top of the Upper Tay (Upper Tay Sandstone C), which is typically a blocky, high net-to-gross sandstone with excellent reservoir quality (Fig. 5). This blocky sandstone unit appears to be relatively continuous in the Pilot–Blakeney area, present in all wells within the Composite Terrace area and pinching out on to the slope of the Moussa delta-complex to the west. It is interpreted as a lowstand systems tract deposit and has better reservoir properties than most of the Tay Sandstone Member in this area. The Pilot Field is well appraised with a total of five wells and two sidetracks, whereas the remaining discoveries are confirmed by an exploration well each.

The seismic expression of Pilot, Blakeney and Feugh in time-section is shown in stack reflectivity and rEEIχ27 displays in Figure 7. Feugh stands out clearly in both stack and rEEIχ27 images. Pilot and Blakeney are more obvious on the rEEI χ27, but also discernible on the stack (in this line of section) once their location is pointed out. The mapped expression of the Top Tay in two-way time structure and stack amplitude is illustrated in Figure 8a and b, respectively. Identifying fluid type from stack amplitude response alone is problematic. The gas in Feugh, Harbour and eastern Pilot is obvious (orange colours). However, oil in Blakeney and the remaining part of Pilot is not clearly distinguishable from brine-sands (green colours). In contrast, the rEEIχ27 response is definitive (Fig. 8c). Calibration of the rEEIχ27 results to well data allows for establishing the thresholds at which oil, gas and brine are indicated. On a horizon slice display it becomes possible to make a number of significant observations.

(1) Whilst the western stratigraphic pinch-out of Pilot had previously been mapped using seismic amplitude data calibrated to an appraisal well (21/27-3), the northern pinch-out closure was more challenging to locate and was sensitive to which seismic volume was used. Stratigraphic pinch-out had previously been suspected in this area but the inversion allows for a practical method of determining the location and changes in pay thickness as pinch-out is approached.
(2) The feeder canyons to Pilot are indicated to be largely oil-bearing. These features were previously regarded as a prospective resource but can now be targeted with more confidence. Furthermore, the feeder canyon midway between Pilot South and Pilot Main (separate oil–water contacts) is clearly connected only to Pilot Main. Pilot South is connected to the southernmost feeder canyon. This observation goes a long way to explaining the *c.* 30 m difference in oil–water contact between the Pilot Main and South accumulations, something that was previously not as well defined or understood.
(3) Blakeney is confirmed as entirely dip closed and filled to spill. Calibration of the dip closure with the oil–water contact in the well furthermore allows for the calculation of the pay thickness required for identification of an oil response using rEEIχ27 in this area. It is established as 8 m, which is approximately equal to one quarter of the seismic wavelength. The oil anomaly sits comfortably within the mapped dip closure because it falls below resolution as the spill point is approached.
(4) A number of amplitude brights to the east of Pilot Main had previously been interpreted as gas accumulations, with an underlying oil leg suspected as encountered in Harbour (27/21-1), the most eastern of them. With the rEEIχ27 data, the oil legs can now be very clearly imaged. The Harbour discovery, its northern extension and the associated small prospects (Fig. 8c) are considered non-commercial, but this demonstrates the resolution of the technique.

The characterization of brine-, oil- and gas-bearing sandstones is illustrated in cross-plots of acoustic impedance v. gradient

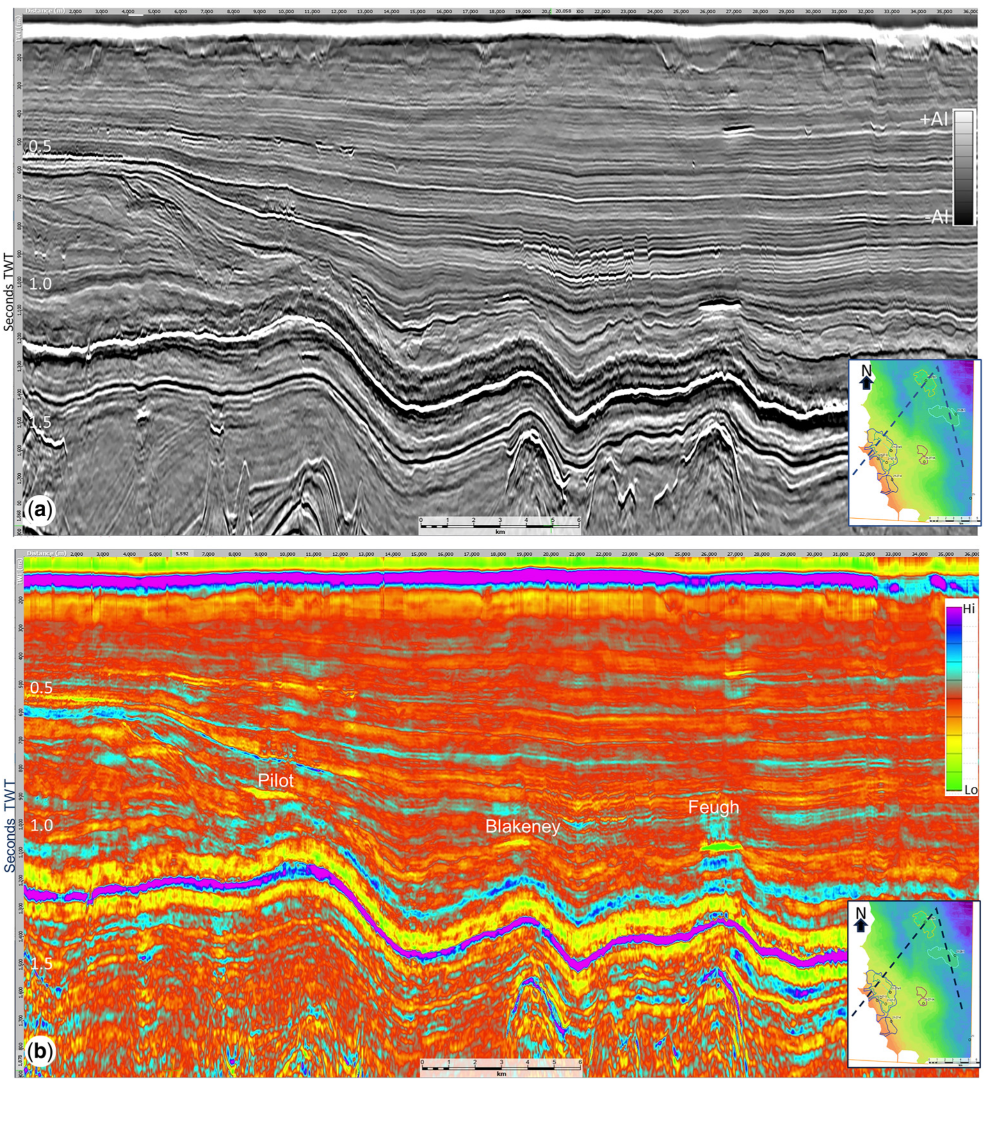

Fig. 7. Arbitrary line through Pilot, Blakeney and Feugh discoveries: (**a**) stack reflectivity; (**b**) rEEIχ27.

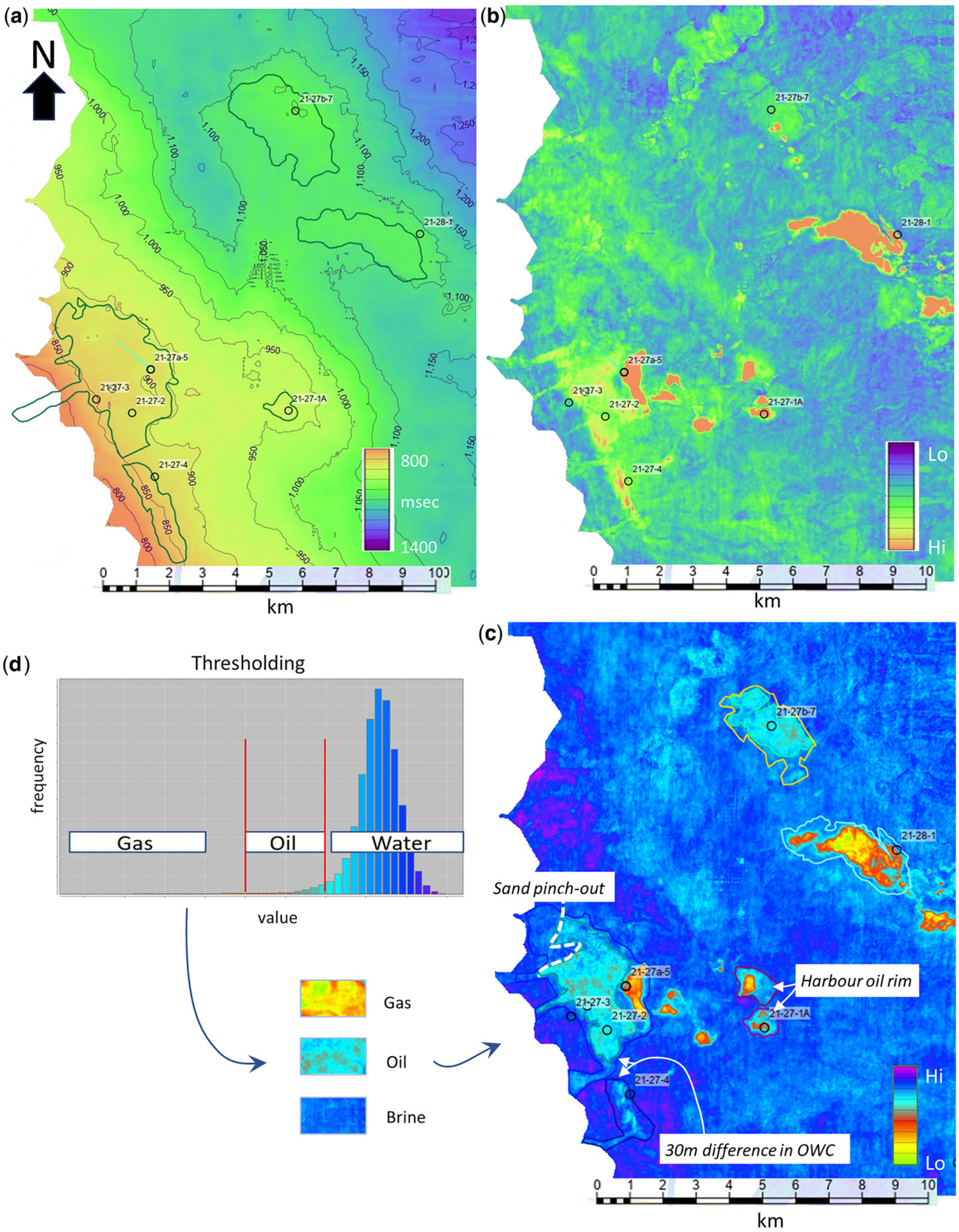

Fig. 8. (**a**) Top Tay two-way time map with scout outlines of the existing discoveries showing a broad conformance with structural elevation; (**b**) stack amplitude extraction (absolute maximum amplitude) from a window (−5 to +20 ms) around Top Tay; (**c**) rEEIχ27 (absolute minimum) attribute extraction from a window (−5 to +20 ms) around Top Tay; (**d**) thresholding of rEEIχ27 values to characterize gas, oil and brine distribution. OWC, oil–water contact.

impedance, colour coded by rEEIχ27, in Figure 9. An area of background, taken from an area to the SE of Pilot, acts as a control when assessing other areas that may be hydrocarbon bearing. This is backed up by taking a cube of data at Tay level from the locality of the dry well 21/21-1, drilled *c.* 12 km to the NW of Blakeney, which shows a response similar to the selected background area, confirming the character of a brine response. The heavy oil in Pilot shows as data points plotting further to the SW corner on the AI–GI cross-plot, with the lowest rEEIχ27 values appearing in green, as a Class 2 AVO anomaly. This is characteristic of a heavy oil response in this area, being similar to that at Blakeney (Fig. 6b). The rEEIχ27 oil response is relatively subtle but clearly distinct from the brine response. Of note, the oil is not anomalous in terms of acoustic impedance contrast alone. It shares the same acoustic impedance as much of the background brine data plotting in the yellow and red colours. Hence, oil is not easy to identify on the full stack data. Gas in the Feugh discovery shows a very strong rEEIχ27 response. The anomaly extends far to the SW corner of the cross-plot. It is also anomalous in terms of acoustic impedance, and hence it is also clearly observable on the full stack.

The elastic characteristics described above are determined by the physical properties of the rocks in the subsurface. The Tay sandstone has high compressibility which is greater with an oil fill. The greater compressibility (lower AI compared with the brine case) results in lower V_p/V_s, since shear impedance is not significantly altered by any change in fluid fill. The lower V_p/V_s systematically changes the gradient, and together with the lowered AI, results in lower EEI values at wide angle. It is only at wide angle (θ45°, χ27°) that oil sands can be reliably discriminated from brine sands and shales (Fig. 6).

Fyne area results

The Tay Sandstone Member in the Fyne area is very different to that seen in the Pilot–Blakeney area. The depth to Top Tay increases progressively from Feugh to Guillemot in the east (Figs 4 & 10). The thickness of the Tay Sandstone Member also increases but wireline log suites confirm it becomes a significantly lower net-to-gross system, with thinner sandbodies, each typically less than 5 m thick, interbedded with shales (Fig. 11). The change is attributed to an increase in the slope in the Fyne area, thus creating

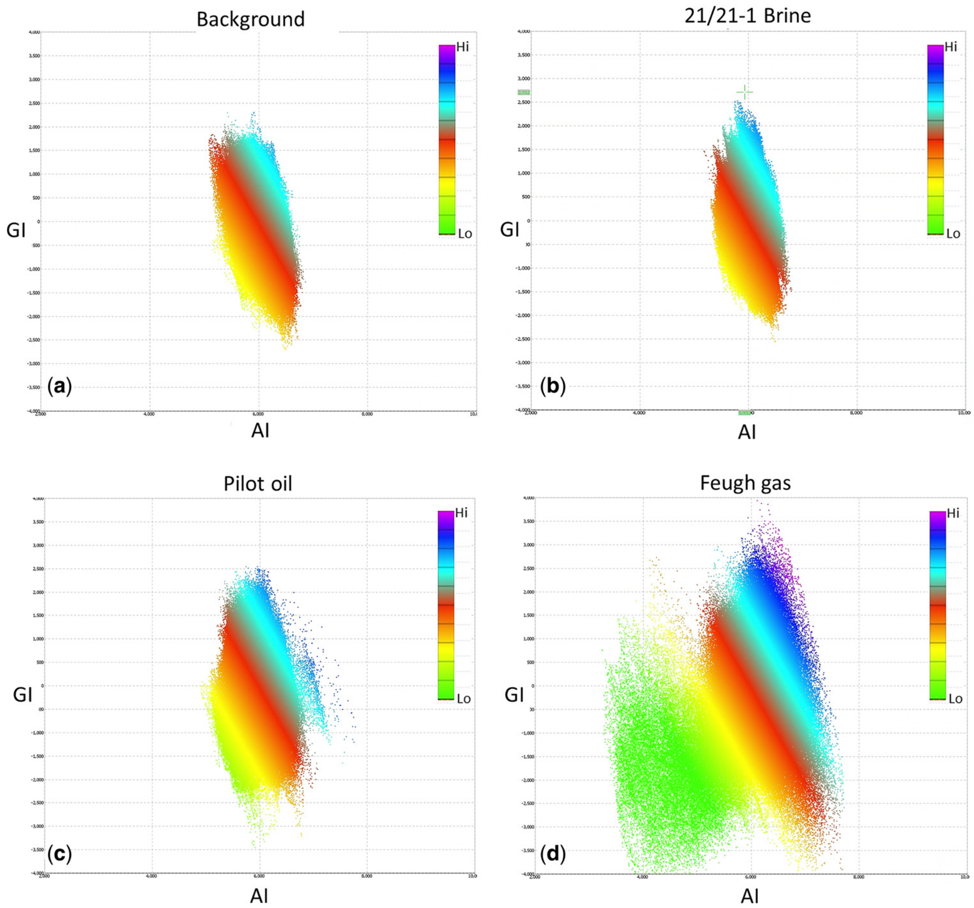

Fig. 9. AI–GI cross-plots, colour coded by rEEIχ27, obtained from cubes of data in the greater Pilot area: (**a**) background (brine) control from area to SE of Pilot; (**b**) dry hole (brine) response from 21/21-1; (**c**) Pilot oil response; (**d**) Feugh gas response. The oil–brine threshold in Figure 7 corresponds to the change from yellow to green colours in rEEIχ27.

channel systems that are largely bypass zones, supplying vast amounts of Tay sands to the basin floor where the Gannet and Guillemot fields are located (Jones *et al.* 2003).

Well results confirm that the Tay Sandstone is not present everywhere on the slope, being replaced by Horda Formation mudstones, indicating that the sand fairways are laterally restricted. The rEEIχ27 attribute proves useful for identifying the sand fairways on the slope (Fig. 12). The presence of hydrocarbon-filled sands (typically gas in thin sands) at the top of the Tay is clearly defined for the fairway connecting Feugh, at the top of the slope, with Guillemot and NW Guillemot which are located on the basin floor. The well data confirm the fidelity of the attribute and furthermore suggest that although the attribute is from the Top Tay, the sand fairway was fixed in position throughout the period of Tay deposition. With the much lower net-to-gross Tay system and the absence of the Upper Tay Sandstone C reservoir unit, hydrocarbons are no longer focused exclusively in the Upper Tay, but tend to occur in the upper parts of the section wherever sands are developed in the member.

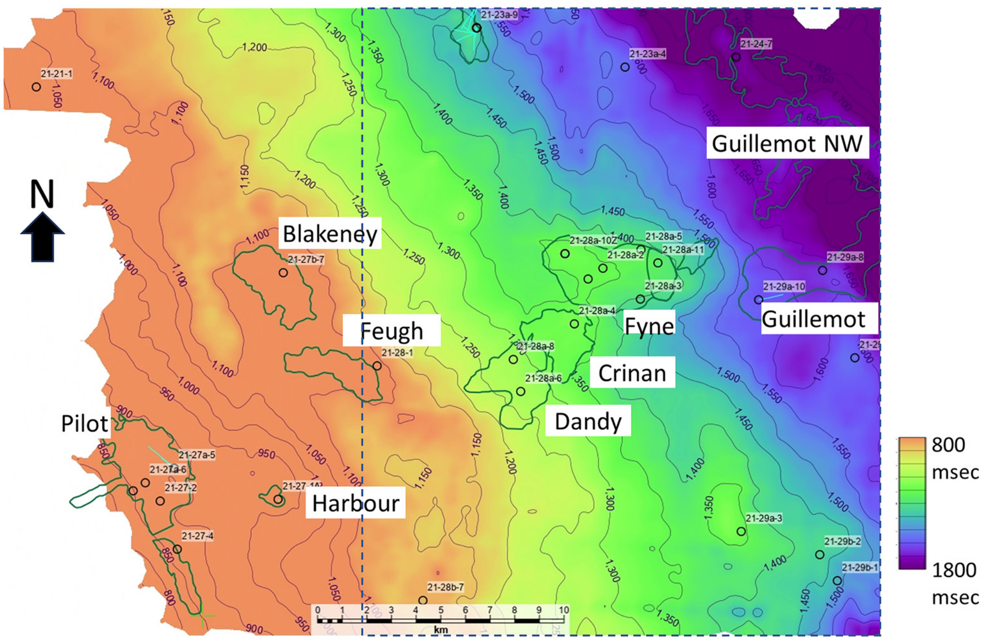

Fig. 10. Top Tay structure in two-way time, illustrating the more basinward positions of Dandy, Crinan, Fyne and Guillemot.

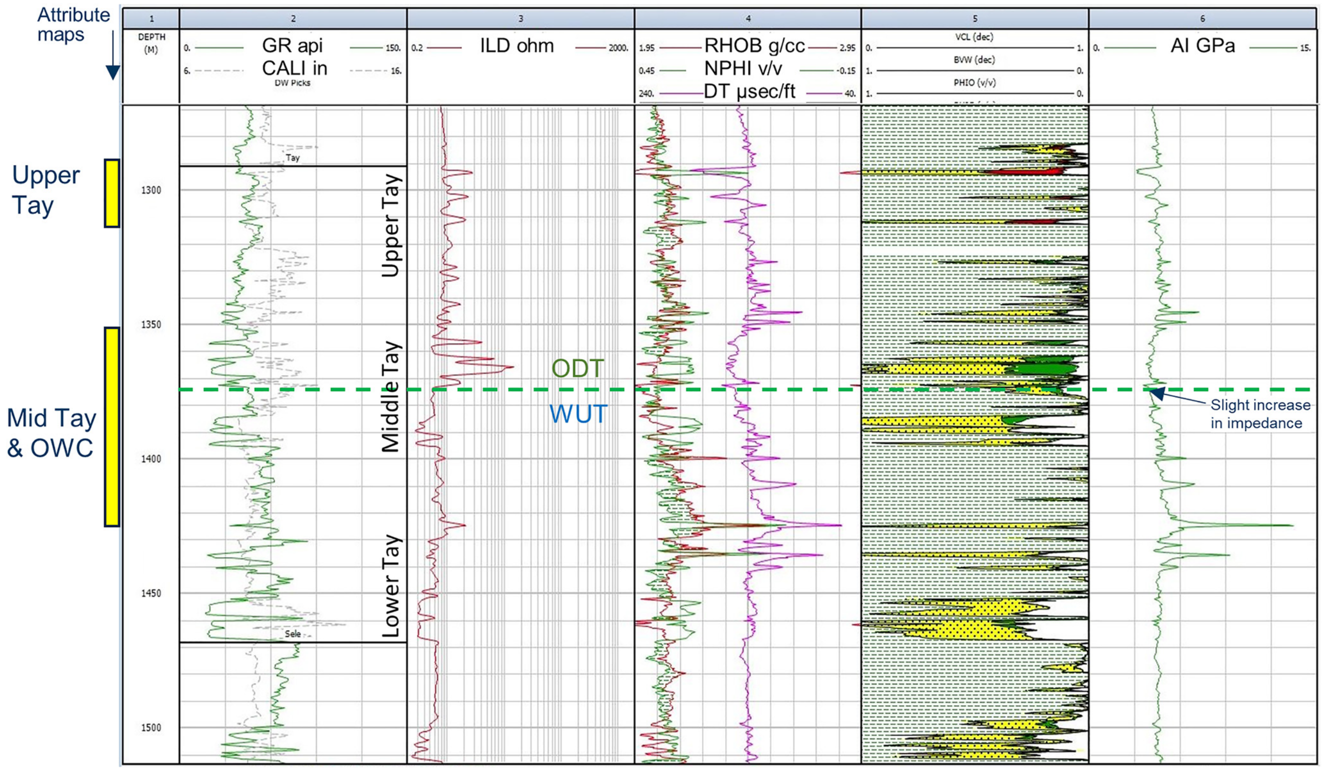

Fig. 11. Well logs from Crinan discovery well 21/28-4. The total Tay interval is around 160 m thick. The Upper Tay shows gas in thin sands. The Middle Tay is an interval of higher net-to-gross with sands both above and below the interpreted oil–water contact (OWC). The Lower Tay also shows higher net-to-gross but is brine-filled. The approximate position of the seismic attribute extractions discussed in the text is shown on the left of the image. The upper attribute aims to show the location of hydrocarbon-bearing sands at Top Tay. The Middle Tay attribute aims to identify areas of better net-to-gross above the OWC in the Middle Tay section. ODT, oil down to; WUT, water up to.

The Fyne discovery sits above a salt swell, is appraised by multiple wells, yet remains undeveloped. The reason for this is the mixed appraisal drilling results, particularly the sporadic lack of high net-to-gross reservoir above the oil–water contact in the main Middle Tay interval, which is the target pay zone in Fyne. As a result of individual oil-sands being below seismic resolution and thin gas-sands occurring above the main oil pay interval, seismic data have typically been considered incapable of resolving net-to-gross variations in the Middle Tay.

Given the difficulty in mapping the Middle Tay as a horizon, we have investigated mapping net-to-gross using a knowledge of the rock properties and the location of the oil–water contact as a potential way forward (Fig. 13). The Tay is typically 150 m thick and the Middle Tay sits *c.* 50 m below the Top Tay. The oil–water contact sits *c.* 85 m below the Top Tay, where penetrated by wells in the main part of the field but is obviously less distant from Top Tay towards the margins of any structural closure. When investigating AVO behaviour we normally think of the relationship between the cap rock and the top of the reservoir, where we look for a change to softer elastic attributes (e.g. EEIχ27) in the reservoir to indicate the presence of hydrocarbons. At the oil–water contact the opposite effect is observed (Fig. 13b). Here we expect a 'hard kick' (increase in rEEIχ27), if good soft oil-sands are underlain by hard brine-sands.

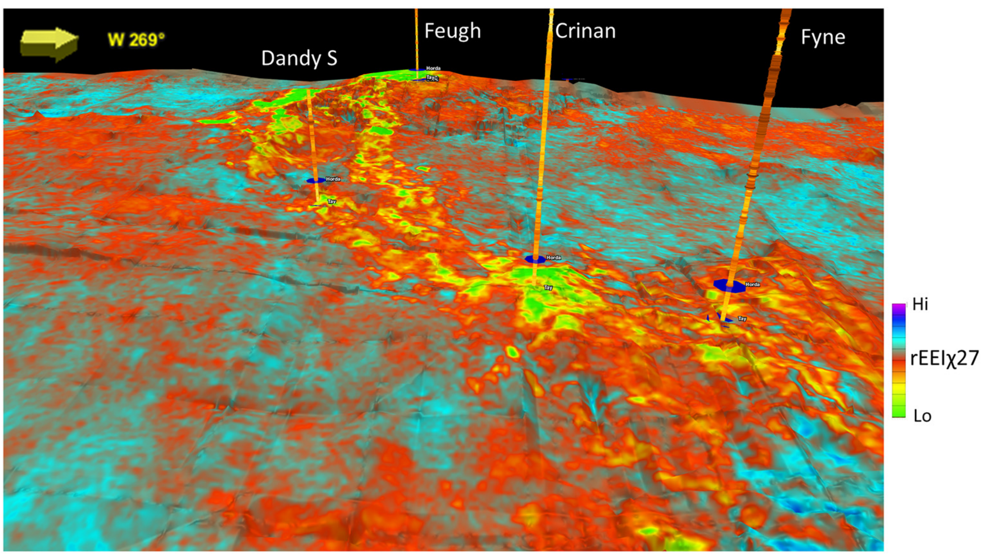

Fig. 12. Top Tay structure in perspective view looking to the west from Fyne to Feugh. The attribute rEEIχ27 is draped on the Top Tay two-way time surface. The attribute is obtained from a window −5 to +20 ms around Top Tay. The yellow–green represents low values of rEEIχ27 associated with hydrocarbon-filled sandstones. The blue–red represents mid-case values associated with mudstone. Hence the attribute picks out the sand fairway, which is also the hydrocarbon migration fairway. Oil and gas progressively fills and spills structures up the fairway from Fyne to Feugh.

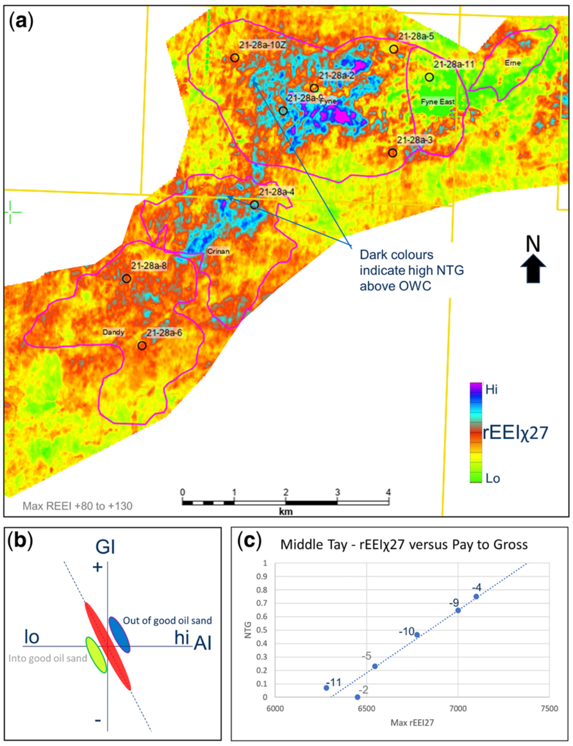

Fig. 13. (**a**) Seismic attribute showing maximum rEEIχ27 in a 50 ms interval +80 to +130 ms below Top Tay. The dark blue colours represent high values of rEEIχ27 and are prognosed to indicate where better net-to-gross (NTG) exists above the oil–water contact (OWC) in the Middle Tay. (**b**) The blue ellipse on the AI–GI cross-plot shows the expected high values of rEEI (hard kick) where soft oil-sands pass to hard brine-sands below the OWC. (**c**) A positive correlation exists between pay to gross (oil-bearing NTG) and maximum rEEIχ27, at well locations, suggesting the method has merit in determining areas of better reservoir in the Fyne–Crinan area. Note, the attribute did not adequately sample the Middle Tay in wells −2 and −5.

On the other hand, if there are low net-to-gross sands above the oil–water contact, we do not expect a very hard kick since the response will be dominated by shale rather than the oil-sands, and a more muted response will instead result. The AVO prediction in this case is based on first principles rather than any quantitative modelling. However, a cross-plot of maximum rEEIχ27 v. oil-bearing net-to-gross (pay to gross) from the wells in Crinan and Fyne at the level of the Middle Tay shows a good positive correlation, suggesting the method may have merit for reservoir characterization and well planning (Fig. 13c). Examination of an arbitrary line running through the discovery wells on this fairway further highlights the coincidence of a downwards increase in rEEIχ27 at, or near, the oil–water contacts at Erne, Fyne, Crinan and Dandy; the higher values of rEEIχ27 (darker blues) correspond with the highest net-to-gross above the oil–water contact (Fig. 14).

Screening for additional prospects

The gross depositional environment (GDE) map (Fig. 3) was constructed using well and seismic data (Brown *et al.* 2020) but has now been refined with the rEEIχ27 data. Previous sections have focused on the Pilot area on the Composite Terrace and the Fyne Secondary Slope channel system. A comparable slope channel system links from the Composite Terrace to Sheryl, Pict and Saxon in the north. To the south, the Composite Terrace (transient basin) is not developed and a simpler system exists with Elke and Narwhal linking down a longer, more gradual slope, to Belinda on the basin floor. It is important to note that the slope channel systems define not only the sand fairways, but also the hydrocarbon migration pathway. Hence, an important step in de-risking a prospect is that they should lie on a charge route related to one of these fairways.

The Dee prospect lies on the Fyne–Crinan–Dandy–Feugh sand and hydrocarbon migration fairway. The prospect has a prominent gas anomaly, highly indicative of hydrocarbon charge (Figs 14 & 15). The discoveries along this fairway all contain gas over oil

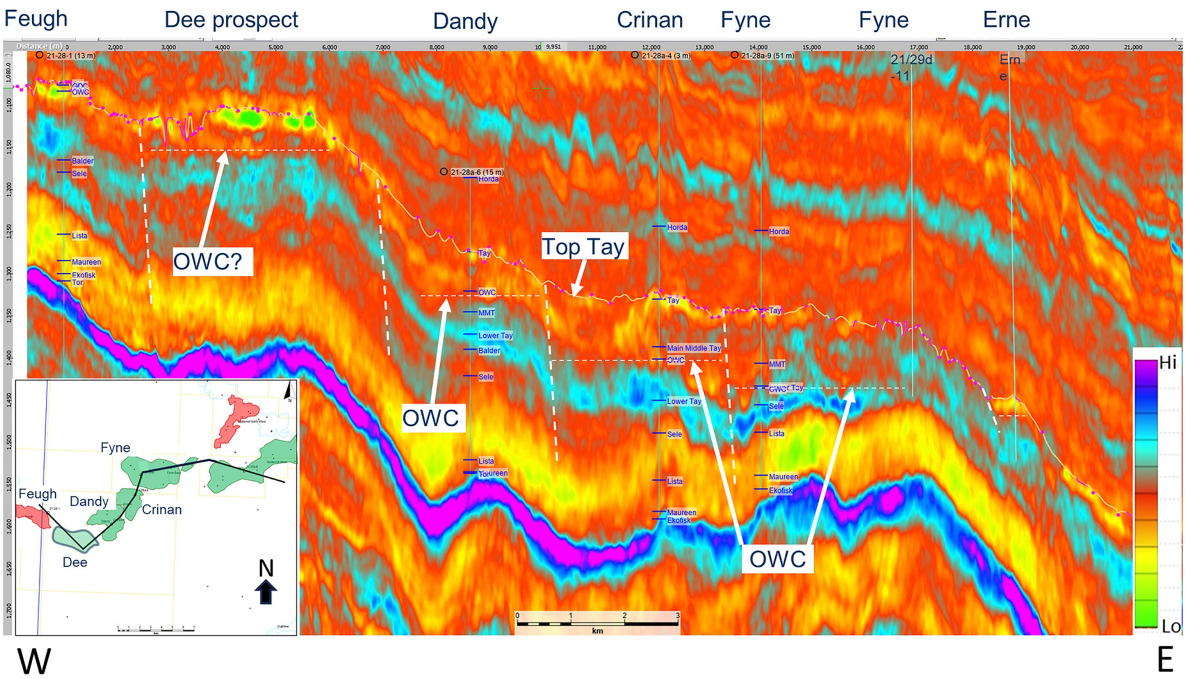

Fig. 14. Arbitrary line showing the rEEIχ27 attribute through discoveries between Feugh and Guillemot. The Top Tay is typically recorded as a decrease in rEEIχ27 reflecting the presence of gas in the thin Upper Tay sandstones. There is a prominent change to hard rEEIχ27 (blue) at the oil–water contact (OWC) in the different discoveries (horizontal white dotted lines). The dark blue at the OWC in Crinan and West Fyne records high net-to-gross above the OWC. East Fyne has very low net-to-gross through the Tay with no OWC detected by the attribute. The OWC is picked out by the attribute in Dandy and Erne. Another prominent flat surface with the downward change to a hard kick (blue) colours exists in the Dee prospect. Dee contains a prominent gas cap at Top Tay but with a considerable space beneath the gas bright and the possible OWC suggesting the potential for a significant column of oil. The sub-vertical white dashed lines mark the mapped boundaries of the discoveries.

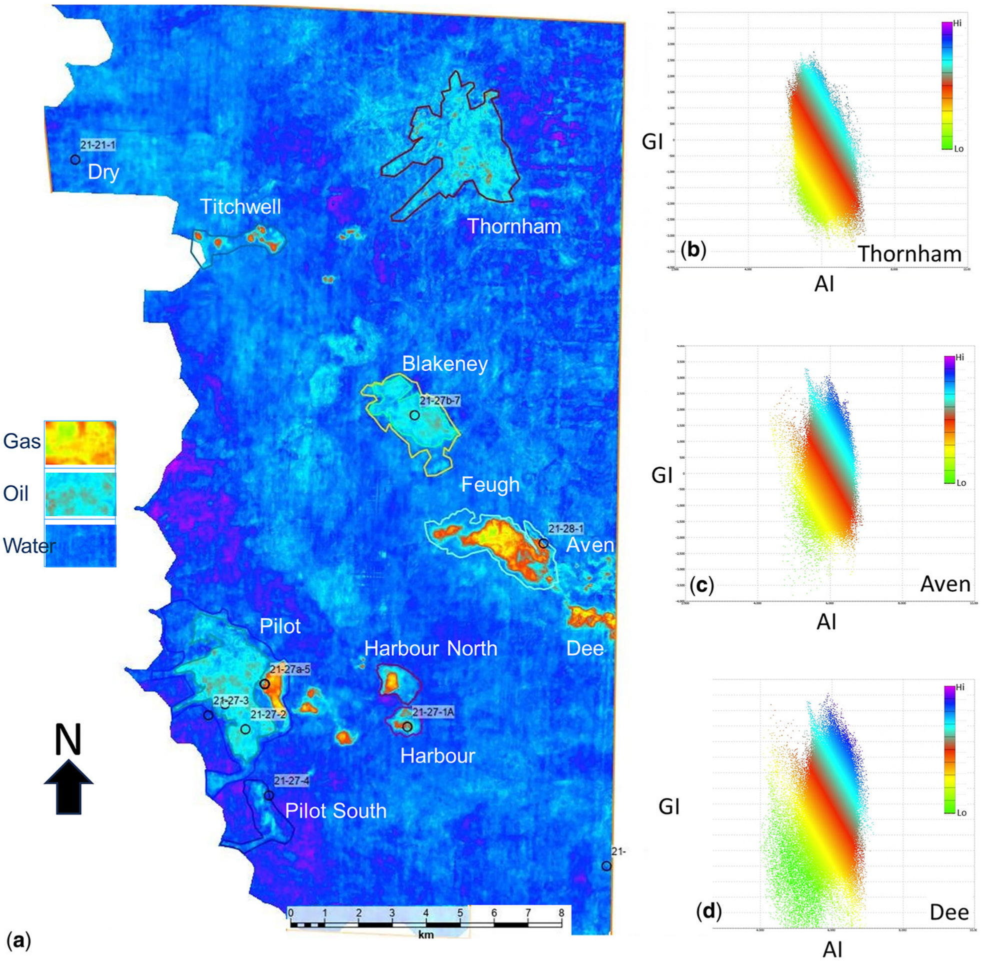

Fig. 15. (**a**) Horizon slice of rEEIχ27 from a window −5 to +20 ms around Top Tay, showing the hydrocarbon anomalies proved by wells in Harbour, Blakeney, Feugh and Pilot and the undrilled anomalies at Harbour North, Thornham, Aven and Dee. (**b–d**) AI v. GI cross-plots showing the rEEIχ27 anomalies at Thornham, Aven and Dee. AI–GI cross-plots are scaled the same as the plots in Figure 9.

and Dee is prognosed likewise. The main risks are reservoir net-to-gross and oil column height, the latter most probably determined by lateral seal competence. Aven has a similar, but less gas-prone rEEIχ27 anomaly and is separated from Dee by a late-stage mud-filled channel deposit. The same mud-filled channel also separates Dandy into Dandy North (21/28a-6) and Dandy South (21/28a-8) which show different oil–water contacts (Figs 12 & 15).

The Thornham prospect lies in a comparable position to Dee at the up-dip limit of a slope channel system running through Pict, Saxon and Sheryl (Fig. 3). It shows an rEEIχ27 anomaly, the down-dip part of which conforms with two-way time. The up-dip parts suggest channels that may seal for oil but not for gas, since gas-brights further up-dip are on trend with the channels and form part of the Titchwell lead. The main risk is perceived to be up-dip seal.

In addition to high-grading existing and new prospectivity, other prospects have been down-graded, either as a result of the absence of an oil-response, or a weak oil-type response probably indicative of thin pay which carries commercial risk in a heavy oil development.

Conclusions

Elastic inversion of recently reprocessed seismic data in the Pilot–Blakeney area has been used to successfully delineate oil distribution in high net-to-gross discoveries in the Pilot–Blakeney area, and in the low net-to-gross discoveries in the Fyne, Crinan and Dandy areas.

Well log data were first used to assess the potential for discriminating fluid type and sand quality from seismic attributes. Forward modelling from well log studies suggested an attribute derived from intercept (I) and gradient (G), representing an I–G cross-plot rotation angle (χ) of 27°, would be ideal for fluid discrimination. The attribute, relative extended elastic impedance (rEEIχ27), was generated from partial angle stacks and relative impedance inversion. The attribute was then blind tested to see if it could identify hydrocarbons directly, which it did with a high degree of fidelity. The approach used is one that relies entirely on the information contained within the seismic data to identify lithology and fluid. Wells are not used in the inversion but are instead used to test the efficacy of the method.

The method has proved robust for delimiting heavy oil pay where the column is greater than 8 m thick. This is useful in a heavy oil setting where thin beds are non-commercial. Gas over oil, oil and brine-filled sands can each be discriminated from one another using rEEIχ27. However, brine-sands cannot be easily discriminated from shales, a feature predicted by the well data and deduced to be due to the comparable elastic properties of the sand and shale in the study area, which in turn relates to the shallow depth of burial and limited compaction. Oil and gas, trapped further down-dip in the discoveries of Fyne, Crinan and Dandy, are present in Tay reservoirs with lower net-to-gross. The rEEIχ27 attribute, in this case, is shown to be sensitive to the presence of higher net-to-gross in the oil leg, a characteristic of direct relevance to the planning of optimally located development wells.

Acknowledgements The constructive reviews of Paul Howlett and Mark Attree, and the guidance of editor Graham Goffey, are each gratefully acknowledged. TGS and Orcadian are thanked for permission to publish. Special thanks are extended to Aliya Shikhullaeva and Sadie Holmes for their diligent work conducted through reprocessing of the seismic data.

Competing interest The authors declare that they have no known competing financial interests or personal relationships that could have appeared to influence the work reported in this paper.

Author contributions **DW**: conceptualization (lead), formal analysis (lead), investigation (lead), methodology (lead), validation (lead), writing – original draft (lead), writing – review & editing (lead); **MB**: formal analysis (equal), investigation (equal), writing – original draft (supporting), writing – review & editing (equal); **JR**: formal analysis (equal), investigation (equal), visualization (supporting); **SB**: funding acquisition (equal); **GT**: funding acquisition (lead), project administration (lead).

Funding This research received no specific grant from any funding agency in the public, commercial, or not-for-profit sectors.

Data availability The data that support the findings of this study are available from TGS Geophysical ASA, but restrictions apply to the availability of these data, which were used under licence for the current study, and so are not publicly available. Data are, however, available from the authors upon reasonable request and with permission of TGS Geophysical ASA.

References

Adeogba, A.A., McHargue, T.R. and Graham, S.A. 2005. Transient fan architecture and depositional controls from near-surface 3-D seismic data, Niger Delta continental slope. *AAPG Bulletin*, **89**, 627–643, https://doi.org/10.1306/11200404025

Brown, S.A., Wood, P.H., Bamford, M.L.F. and Gluyas, J.G. 2020. The Pilot, Elke, Blakeney, Narwhal, Harbour and Feugh fields, Blocks 21/27, 21/28, 28/2 and 28/3, UK North Sea. *Geological Society, London, Memoirs*, **52**, 560–573, https://doi.org/10.1144/M52-2017-25

Castagna, J.P. and Swan, H.W. 1997. Principles of AVO crossplotting. *The Leading Edge*, **16**, 337–344, https://doi.org/10.1190/1.1437626

Fatti, J.L., Smith, G.C., Vail, P.J., Strauss, P.J. and Levitt, P.R. 1994. Detection of gas in sandstone reservoirs using AVO analysis: A 3-D seismic case history using the Geostack technique. *Geophysics*, **59**, 1362–1376, https://doi.org/10.1190/1.1443695

Gidlow, P.M., Smith, G.C. and Vail, P. 1993. Hydrocarbon detection using fluid factor traces: a case study. *3rd SAGA Biennial Conference and Exhibition*, April 1993, Cape Town, South Africa, Abstracts, 224, https://doi.org/10.3997/2214-4609-pdb.224.041

Greenberg, M.L. and Castagna, J.P. 1992. Shear-wave velocity estimation in porous rocks: Theoretical formulation, preliminary verification and applications. *Geophysical Prospecting*, **40**, 195–209, https://doi.org/10.1111/j.1365-2478.1992.tb00371.x

Jones, E., Jones, R. *et al*. 2003. Eocene. *In*: Evans, D., Graham, C., Armour, A. and Bathurst, P. (eds) *The Millennium Atlas: Petroleum Geology of the Central and Northern North Sea*. Geological Society, London, 261–277.

Knox, R.W.O'B. and Holloway, S. 1992. *Lithostratigraphic Nomenclature of the UK North Sea: Paleogene of the Central and Northern North Sea*. British Geological Survey.

Mur, A. and Vernik, L. 2019. Testing popular rock-physics models. *The Leading Edge*, **38**, 350–357, https://doi.org/10.1190/tle38050350.1

Rutherford, S.R. and Williams, R.H. 1989. Amplitude-versus-offset variations in gas sands. *Geophysics*, **54**, 680–688, https://doi.org/10.1190/1.1442696

Smith, G.C. and Gidlow, P.M. 1987. Weighted stacking for rock property estimation and detection of gas. *Geophysical Prospecting*, **35**, 993–1014, https://doi.org/10.1111/j.1365-2478.1987.tb00856.x

Vernik, L. 2016. *Seismic Petrophysics in Quantitative Interpretation*. Society of Exploration Geophysicists, Investigations in Geophysics, **18**, https://doi.org/10.1190/1.9781560803256

Went, D.J. 2021. Practical application of global siliciclastic rock-property trends to AVA interpretation in frontier basins. *The Leading Edge*, **40**, 454–459, https://doi.org/10.1190/tle40060454.1

Went, D.J., Hedley, R. and Rogers, J. 2023. Screening for AVA anomalies in siliciclastic basins: testing a seismic inversion method in the Mississippi Canyon, Gulf of Mexico. *First Break*, **41**, 75–81, https://doi.org/10.3997/1365-2397.fb2023076

Whitcombe, D.N., Connolly, P.A., Reagan, R.L. and Redshaw, T.C. 2002. Extended elastic impedance for fluid and lithology prediction. *Geophysics*, **67**, 63–67, https://doi.org/10.1190/1.1451337